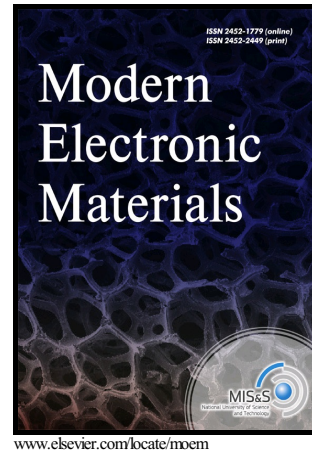


# Author's Accepted Manuscript

Structural properties of the formation of zinc-containing nanoparticles obtained by ion implantation in Si (001) and subsequent thermal annealing

Ksenia B. Eidelman, Nataliya Yu. Tabachkova, Kirill D. Shcherbachev, Yuri N. Parkhomenko, Vladimir V. Privesentsev, Denis M. Migunov



PII: S2452-1779(17)30074-9  
DOI: <https://doi.org/10.1016/j.moem.2017.10.003>  
Reference: MOEM68

To appear in: *Modern Electronic Materials*

Received date: 11 September 2017

Accepted date: 25 October 2017

Cite this article as: Ksenia B. Eidelman, Nataliya Yu. Tabachkova, Kirill D. Shcherbachev, Yuri N. Parkhomenko, Vladimir V. Privesentsev and Denis M. Migunov, Structural properties of the formation of zinc-containing nanoparticles obtained by ion implantation in Si (001) and subsequent thermal annealing, *Modern Electronic Materials*, <https://doi.org/10.1016/j.moem.2017.10.003>

This is a PDF file of an unedited manuscript that has been accepted for publication. As a service to our customers we are providing this early version of the manuscript. The manuscript will undergo copyediting, typesetting, and review of the resulting galley proof before it is published in its final citable form. Please note that during the production process errors may be discovered which could affect the content, and all legal disclaimers that apply to the journal pertain.

# Structural properties of the formation of zinc-containing nanoparticles obtained by ion implantation in Si (001) and subsequent thermal annealing

Ksenia B. Eidelman<sup>1</sup>, Nataliya Yu. Tabachkova<sup>1</sup>, Kirill D. Shcherbachev<sup>1</sup>, Yuri N. Parkhomenko<sup>1</sup>, Vladimir V. Privesentsev<sup>2</sup>, Denis M. Migunov<sup>3</sup>

Corresponding author — Ksenia B. Eidelman, e-mail: eidelman@live.ru

<sup>1</sup>National University of Science and Technology MISiS,

4 Leninsky Prospekt, Moscow 119049, Russia,

<sup>2</sup>Physical and Technological Institute of the Russian Academy of Sciences,

34 Nakhimovsky Prospekt, Moscow 117218, Russia,

<sup>3</sup>National Research University of Electronic Technology (MIET),

1 Shokin Sq., Zelenograd, Moscow 124498, Russia

**K. B. Eidelman<sup>1</sup>**: Assistant (eidelman@live.ru); **N. Yu Tabachkova<sup>1</sup>**: Cand. Sci (Phys.-Math.), Assistant Professor (ntabachkova@gmail.com); **K. D. Scherbachev<sup>1</sup>**: Cand. Sci (Phys.-Math.), Lead Engineer (chtrb@gmail.com); **Yu. N. Parkhomenko<sup>1</sup>**: Dr. Sci. (Phys.-Math.), Professor, Head of Department of the Material Science of Semiconductors and Dielectrics (e-mail parkh@rambler.ru); **V. V. Privesentsev<sup>2</sup>**: Cand. Sci (Eng.), Senior Researcher (v.privezentsev@mail.ru); **D. M. Migunov<sup>3</sup>**: Cand. Sci (Eng.), Lead Engineer, (climbden@gmail.com)

**Abstract.** This work deals with the study of structural transformations in the near-surface layers of silicon after ion beam synthesis of zinc-containing nanoparticles. Phase formation after

ACCEPTED MANUSCRIPT  
implantation of  $Zn^+$  ions and two-stage implantation of  $O^+$  and  $Zn^+$  ions with subsequent thermal annealing in an atmosphere of dry oxygen has been considered. We heated the substrate to 350 °C during the implantation to avoid amorphization. After implantation, the specimens were annealed for 1 h in a dry oxygen atmosphere at 800 °C. Investigation of the structure of surface silicon layers has been carried out by X-ray diffractometry and transmission electron microscopy.

We show that a damaged layer with a large concentration of radiation induced defects forms near the surface as a result of the implantation of  $Zn^+$  ions with an energy of 50 keV. In the as-implanted state, nanoparticles of metallic Zn with a size of about 25 nm form at a depth of 40 nm inside the damaged silicon layer. Subsequent annealing at 800 °C in a dry oxygen atmosphere leads to structural changes in the defect layer and the formation of  $Zn_2SiO_4$  nanoparticles at a depth of 25 nm with an average size of 3 nm, as well as oxidation of the existing Zn particles to the  $Zn_2SiO_4$  phase. The oxidation of the metallic Zn nanoparticles starts from the surface of the particles and leads to the formation of particles with a “core-shell” structure. Analysis of the phase composition of the silicon layer after two-stage implantation with  $O^+$  and  $Zn^+$  ions showed that Zn and  $Zn_2SiO_4$  particles form in the as-implanted state. Subsequent annealing at 800 °C in a dry oxygen atmosphere leads to an increase in the particle size but does not change the phase composition of the near-surface layer. ZnO nanoparticles were not observed under these experimental conditions of ion beam synthesis.

**Keywords:** Ion implantation; Zinc-containing nanoparticles; Core-shell nanoparticles; Willemite

## Introduction

Silicon is the main material of semiconductor electronics. One recent nanoelectronics development trend is the formation of silicon base heterostructures. Zinc oxide ZnO and zinc silicate  $Zn_2SiO_4$  are wide band semiconductors that can be doped for producing either discrete *p*-

$n$  junctions or inside any matrices. Therefore the phase formation of zinc containing nanoparticles in silicon is an important research area for the improvement of heterojunction based devices.

Zinc containing nanoparticles such as ZnO and Zn<sub>2</sub>SiO<sub>4</sub> have good practical capabilities. For example, ZnO base structures are of a great interest because of their potential optoelectronics applications as light emitting diodes [1], random lasers [2] and self-arranging resonator laser structures [3]. Zinc silicate exhibits highly efficient luminescence, high chemical and thermal stability and high nuclear radiation resistance. This material has been widely studied for scintillator applications [4, 5]. Zn<sub>2</sub>SiO<sub>4</sub> based scintillators show good promise for radiation control. Due to their chemical and thermal stability zinc silicates can also be used in corrosive and hot media and under severe radiation exposure [5]. One more zinc silicate application is a humidity gage [6]. Thin Zn<sub>2</sub>SiO<sub>4</sub> films are highly moisture sensitive and exhibit high efficiency and durability. Furthermore, Mn doped Zn<sub>2</sub>SiO<sub>4</sub> is a well-known luminescent material [7]. Depending on the synthesis conditions, doped zinc silicate nanoparticles may contain different numbers of charge traps which can be filled under UV excitation. This causes phosphorescence if the traps are shallow or photostimulated luminescence if the traps are deep and undergo photostimulation [8, 9]. An important advantage of these luminophores is the easily detectable background due to the absence of specimen fluorescence under IR or red irradiation [10].

There are different zinc containing structure synthesis methods:

- sol gel technology [9];
- hydrothermal deposition [10–11];
- molecular beam epitaxy [12–13];
- ion implantation [14–20].

Sol gel technology is the simplest nanoparticle synthesis method but has a significant drawback: its results and surface deposition are poorly reproducible. Along with the sol gel technology, methods that combine material synthesis and deposition also show good promise. Hydrothermal deposition and molecular beam epitaxy are good for semiconductor technologies but their

ACCEPTED MANUSCRIPT

application is generally limited to surface layers. Ion implantation is perfect if a structure is to be synthesized in the bulk of a semiconductor matrix. It allows synthesizing nanoparticles of various compositions and sizes at required depths from the substrate surface [15]. ZnO nanostructure formation by ion implantation and thermal oxidation was studied in numerous works. Most of the experiments dealt with Zn ion implantation into dielectric matrices ( $\text{SiO}_2$ ) followed by thermal annealing in an oxygen atmosphere [21–24]. With these process parameters the experiments resulted in the formation of the ZnO and  $\text{Zn}_2\text{SiO}_4$  phases. Despite the presence of oxygen in the amorphous matrix the annealing atmosphere and temperature had a large effect on the phase formation. Annealing at 600–700 °C led to the formation of zinc oxide, whereas zinc silicate formed at 800–1000 °C. Some studies dealt with the phase formation of nanoparticles after simultaneous introduction of zinc oxide and oxygen by two-beam implantation into silicon matrices [21]. These experiments also confirmed zinc oxide and silicate formation at the abovementioned temperatures.

Below we present our experimental results on the structural transformations in surface silicon layers after ion beam synthesis of zinc containing nanoparticles. We discuss the phase formation processes that follow  $\text{Zn}^+$  ion implantation and sequential two-stage implantation of  $\text{O}^+$  and  $\text{Zn}^+$  ions with subsequent thermal annealing in a dry oxygen atmosphere.

## Experimental

The test specimens were two fragments of an *n* conductivity type phosphorus doped single crystal silicon wafer with the (001) orientation. One fragment was implanted with  $5 \cdot 10^{16} \text{ cm}^{-2}$   $^{64}\text{Zn}^+$  ions at 50 keV, and the other was sequentially implanted with  $\text{O}^+$  (35 keV,  $5 \cdot 10^{16} \text{ cm}^{-2}$ ) and  $\text{Zn}^+$  (120 keV,  $5 \cdot 10^{16} \text{ cm}^{-2}$ ) ions. A  $\varnothing 2$  mm  $\text{Zn}^+$  and  $\text{O}^+$  ion beam scanned the wafer surface at 7 arc deg. The ion current density was  $j \leq 50 \text{ nA} \cdot \text{cm}^{-2}$  so the wafer heated to within 50 °C above room temperature. To avoid amorphization we heated the target to 350 °C during the implantation. The mean ion projection range  $R_p$  was calculated with the SRIM software [25].  $R_p$

ACCEPTED MANUSCRIPT

was 40 nm for the 50 keV Zn<sup>+</sup> implanted specimen. For the Zn<sup>+</sup> and O<sup>+</sup> implanted specimen we chose the ion energies so to achieve the same Zn<sup>+</sup> and O<sup>+</sup> projection ranges, 115 nm. After the implantation the specimens were heat treated at 800 °C for 1 h in a dry oxygen atmosphere [26]. The specimen structure was examined with high-resolution electron microscopy (TEM) and X-ray diffraction in the Materials Science and Metallurgy Joint Use Center of MISiS. X-ray diffraction analysis was carried out on a D8 Discover (Bruker AXS) multipurpose X-ray diffractometer. The source was a 1.6 kW copper anode X-ray tube ( $\lambda_{\text{CuK}\alpha} = 0.15406$  nm). The diffraction patterns were obtained in a parallel source beam arrangement by  $2\theta$  scanning (detector scanning) from a steady specimen. The X-ray incidence angle was 0.3 arc deg. TEM analysis was conducted on a JEM-2100 instrument at a 200 kV accelerating voltage. The TEM specimens were prepared using FEI's Quanta 3D FEG two-beam system at the Joint Use Center for Microsystem Engineering and Electronics Components of the National Research University of Electronic Technology.

## Results and discussion

*Nanoparticle formation during Zn<sup>+</sup> implantation and subsequent heat treatment.* Figure 1 shows X-ray diffraction patterns of the silicon wafer surface after Zn<sup>+</sup> implantation and annealing at 800 °C in dry oxygen gas. The diffraction patterns suggest that a metallic zinc phase is present in the as-implanted specimen (Fig. 1 *a*). The presence of only the zinc (101) reflections in the diffraction pattern suggests a specific orientation correlation between the silicon matrix and the zinc phase. The average size of the zinc coherent scattering regions as determined from the diffraction band broadening is ~20 nm. After the 800 °C anneal in a dry oxygen atmosphere (Fig. 1 *b*) the surface silicon layer contains two phases, i.e. Zn and Zn<sub>2</sub>SiO<sub>4</sub>. Thus two-stage ion beam synthesis (ion implantation and post-implantation anneal) results in the formation of a new crystalline phase.

ACCEPTED MANUSCRIPT

For a more detailed study of the fine structure in the surface silicon layers after Zn implantation followed by annealing we examined the specimens under a TEM. Figure 2 shows silicon cross-section images and electron diffraction patterns of (a) the as-implanted specimen and (b) the specimen annealed at 800 °C in a dry oxygen atmosphere.

The as-implanted specimen contains a clearly seen damaged surface silicon layer approx. 200 nm in thickness with a high concentration of radiation defects. These defects are difficult for identification due to the lack of a sharp contrast in the images. The surface silicon layer contains Zn particles at an approx. 40 nm depth corresponding to the ion projection range. The diffraction pattern in Fig. 2 a shows that the zinc particles have a specific orientation correlation with the silicon substrate. The average Zn particle size is ~20 nm. The silicon surface and the ~20 nm surface layer contain pores. The pores have anisotropic shapes and are elongated along the surface. The pore sizes vary in the 10–20 nm range in length and 5–10 nm across. SRIM simulation showed that the highest concentration of displaced atoms (Si vacancies) is at a 20 nm depth for these implantation conditions. Therefore one probable cause of pore formation is the radiation diffusion induced vacancy agglomeration in the surface layer [27].

The 800 °C anneal led to structural changes in the defect layer (Fig. 2 b). The thickness of the defect layer did not change after the anneal, remaining ~200 nm, but linear defects formed, i.e. dislocations and dislocation loops. The pores annihilated during the anneal, and the surface became rough. Moreover, oxygen anneal produced an approx. 3 nm thick surface silicon oxide layer. Small 2–5 nm particles formed in the ~25 nm surface silicon layer. Analysis of the high-resolution TEM images showed that these particles are the Zn<sub>2</sub>SiO<sub>4</sub> phase. Large Zn particles in the ~40 nm deep surface silicon layer underwent partial Zn oxidation and Zn<sub>2</sub>SiO<sub>4</sub> phase formation after the 800 °C anneal in oxygen (Fig. 3). Figure 3 a shows a high resolution image of a discrete Zn particle. The plane spacing in the particle is that for the Zn phase. The <0001> zone axis for Zn coincides with the <110> zone axis for Si. In Fig. 3 b and c the plane spacing corresponding to the Zn phase is only observed in the center of the particle, while the plane spacing at the particle surface is 0.315 nm corresponding to the Zn<sub>2</sub>SiO<sub>4</sub> phase (131) plane

spacing. In Fig. 3 *d* the only plane spacing observed in the particle corresponds to the  $\text{Zn}_2\text{SiO}_4$  phase. Thus, particle oxidation starts from the surface (Fig. 3 *b* and *c*) [25] and leads to the formation of core-shell particles. After the anneal the surface silicon layer contained Zn particles, Zn– $\text{Zn}_2\text{SiO}_4$  core-shell particles and completely oxidized particles of the  $\text{Zn}_2\text{SiO}_4$  phase (Fig. 3).

**Formation of nanoparticles in silicon during sequential  $\text{O}^+$  and  $\text{Zn}^+$  ion implantation.** X-ray diffraction study of the phase composition of the surface silicon layer after sequential  $\text{O}^+$  and  $\text{Zn}^+$  ion implantation showed that this implantation produces particles of two phases, i.e. Zn and  $\text{Zn}_2\text{SiO}_4$  (Fig. 4, *a*). The coherent scattering region size as determined from Zn (101) diffraction peak broadening was ~12 nm. Dry oxygen gas annealing did not change the phase composition of the surface silicon layer. The surface silicon layer still contained particles of the two abovementioned phases (Fig. 4 *b*). However, the diffraction peaks broadening due to the anneal suggests that the Zn and  $\text{Zn}_2\text{SiO}_4$  particles became larger. The coherent scattering region size of the as-annealed Zn particles was ~20 nm.

Figure 5 shows TEM images of the surface silicon layers (*a*) after sequential  $\text{O}^+$  and  $\text{Zn}^+$  implantation and (*b*) after annealing at 800 °C in dry oxygen. The specimen had no amorphous layer on the surface after the implantation. The thickness of the as-implanted damaged silicon surface layer with a high radiation defect concentration was ~ 250 nm. 5 to 15 nm sized particles were observed at a depth of approx. 110–120 nm from the surface. The location of the reflections in the diffraction pattern of this area corresponds to the Zn phase. Zn particles are coherent with the Si matrix. The [0001] zone axis for Zn coincides with the [110] zone axis for Si. ~5 nm sized particles were observed at a depth of approx. 35 nm, the phase composition of these particles differing from that of the larger Zn particles located at depths of about 115 nm. High resolution TEM data suggest that the particles observed at ~35 nm correspond to the  $\text{Zn}_2\text{SiO}_4$  phase. Thus, sequential implantation of  $\text{O}^+$  and  $\text{Zn}^+$  ions produces particles of two types in the surface silicon layer, i.e. Zn and  $\text{Zn}_2\text{SiO}_4$ . Particles of different phases are located at different depths from the silicon surface: the Zn particles are located at  $R_p = 115$  nm while the  $\text{Zn}_2\text{SiO}_4$  ones are at ~35

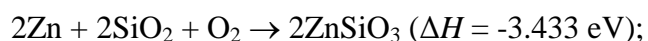
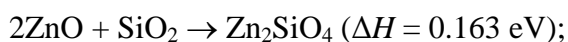
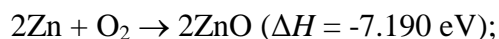


nm. According to the SRIM calculation results this corresponds to the concentration maximum of the displaced atoms. One can assume that the  $Zn_2SiO_4$  particles form in the surface region of the specimen which is rich in silicon. Furthermore, particles of different phases had different sizes. The average size of the Zn particles was 10 nm, and that of the  $Zn_2SiO_4$  particles was 5 nm.

The structure of the defect surface silicon layer changed after dry oxygen anneal at 800 °C for 1 h. The anneal favored the formation of linear defects which can well be seen in Fig. 5 *b*. A ~30 nm thick amorphous  $SiO_2$  layer with amorphous zinc particles formed on the silicon surface. The formation of the amorphous zinc particles in the silicon oxide layer originates from zinc diffusion towards the silicon surface during annealing [28].

The as-annealed surface silicon layer contained Zn and  $Zn_2SiO_4$  particles with a relatively uniform depth distribution in the layer. The as-annealed Zn and  $Zn_2SiO_4$  particle size ranged from 10 to 30 nm. Figure 6 shows high resolution TEM images of discrete particles after (a) sequential implantation of  $O^+$  and  $Zn^+$  ions into silicon and (b) after dry oxygen anneal at 800 °C. Core-shell particles ( $Zn-Zn_2SiO_4$ ) were observed immediately after the sequential implantation (Fig. 6 *a*) and after the anneal (Fig. 6 *b*). After the sequential implantation of  $O^+$  and  $Zn^+$  ions into silicon and dry oxygen anneal the surface silicon layer still contained a large number of metallic zinc particles, whereas after the implantation of  $Zn^+$  ions and subsequent dry oxygen anneal almost all the particles oxidized to  $Zn_2SiO_4$ . This can be attributed to the oxygen diffusion rate being sufficient for the complete Zn particle oxidation at a depth of ~40 nm. During the sequential implantation of  $O^+$  and  $Zn^+$  ions, metallic zinc particles form at a depth of ~115 nm from the surface, and the subsequent anneal causes partial oxidation of the Zn particles to the  $Zn_2SiO_4$  phase. It seems that the oxygen flowrate used in our experiment was insufficient for the complete oxidation of the zinc particles located at ~115 nm from the surface. Noteworthy, neither  $Zn^+$  implantation, nor the subsequent dry oxygen anneal, nor the sequential implantation of  $O^+$  and  $Zn^+$  ions into silicon produced ZnO particles.

According to [29, 30], the Si/Zn/O may have the following phase reactions:



Since the zinc silicate formation is an exothermal reaction ( $\Delta H < 0$ ), this phase is more stable than zinc oxide. The chemical reactions occur in the solid state (the crystalline matrix) under the conditions of major elastic stresses (1 to 10 GPa) and high radiation defect concentrations which may affect the direction of the reactions. The thermodynamic reaction occurs at high temperatures (1000–1300 °C) [28]. If phase formation occurs as a result of ion implantation or after the subsequent thermal oxygen diffusion from the surface, the radiation defects produce local stresses that induce nanoparticle formation processes. Thus,  $\text{Zn}_2\text{SiO}_4$  phase formation at 800 °C is a result of the thermal oxidation on the particle surfaces.

## Summary

We showed that  $5 \cdot 10^{16} \text{ cm}^{-2} \text{ Zn}^+$  ion implantation at 50 keV into a (001) single crystal silicon wafer heated to 350 °C produces metallic ~20 nm sized Zn nanoparticles at a depth of 40 nm. Subsequent anneal at 800 °C in a dry oxygen atmosphere produces  $\text{Zn}_2\text{SiO}_4$  particles with an average size of ~3 nm in the 25 nm deep surface silicon layer and oxidizes the existing Zn particles to  $\text{Zn}_2\text{SiO}_4$ . The oxidation of the Zn nanoparticles starts from the surface and leads to the formation of core—shell type particles.

Two types of nanoparticles form immediately after sequential implantation of  $\text{O}^+$  and  $\text{Zn}^+$  into the silicon matrix, i.e. Zn and  $\text{Zn}_2\text{SiO}_4$ . ~5 nm sized  $\text{Zn}_2\text{SiO}_4$  particles form in the surface silicon

layer at a depth of ~35 nm, and Zn<sup>+</sup> particles with an average size of 10 nm form at a depth of ~115 nm. One can assume that Zn<sub>2</sub>SiO<sub>4</sub> particle formation is favored by silicon vacancies located in the surface region of the specimen. Annealing at 800 °C in a dry oxygen atmosphere increases the particle sizes.

After Zn<sup>+</sup> implantation and dry oxygen anneal almost all the Zn particles in the surface silicon layer oxidized to the Zn<sub>2</sub>SiO<sub>4</sub> phase, whereas after two-stage O<sup>+</sup> and Zn<sup>+</sup> implantation and subsequent anneal the metallic Zn nanoparticles remained in the surface silicon layer. ZnO particles did not form as a result of ion beam synthesis under the experimental conditions.

*The work was accomplished using the equipment of the Joint Use Center for Microsystem Engineering and Electronics Components of the National Research University of Electronic Technology with support from the Ministry of Education and Science of the Russian federation (Grant No. 14.578.21.0188, Agreement Identifier No. RFMEFI57816X0188).*

*The Authors wish to thank Roman Boettger of the Helmholtz Dresden-Rossendorf Research Center (HZSR), Germany, for help with two-stage implantation.*

## References

1. T. Aoki, Y. Hatanaka, D. C. Look, ZnO diode fabricated by excimer-laser doping. *Appl. Phys. Lett.*, 2000, vol. 76, no. 22, pp. 3257. DOI: 10.1063/1.126599
2. H. Cao, Y. G. Zhao, S. T. Ho, E. W. Seelig, Q. H. Wang, R. P. H. Chang, Random laser action in semiconductor powder. *Phys. Rev. Lett.*, 1999, vol. 82, no. 11–15, pp. 2278. DOI: 10.1103/PhysRevLett.82.2278
3. M. Kawasaki, A. Ohtomo, I. Ohkubo, H. Koinuma, Z. K. Tang, P. Yu, G. K. L. Wong, B. P. Zhang, Y. Segawa, Excitonic ultraviolet laser emission at room temperature from naturally made cavity in ZnO nanocrystal thin films. *Materials Science and Engineering: B*, 1998, vol. 56, no. 2–3, pp. 239–245. DOI: 10.1016/S0921-5107(98)00248-7

4. S. Zh. Karazhanov, P. Ravindran, H. Fjellvåg, B. G. Svensson, Electronic structure and optical properties of ZnSiO<sub>3</sub> and Zn<sub>2</sub>SiO<sub>4</sub>. *J. Appl. Phys.*, 2009, vol. 106, no. 12, pp. 123701. DOI: 10.1063/1.3268445
5. Yongning He, Xiaolong Zhao, Xuyang Wang, Liang Chen, Wenbo Peng, Xiaoping Ouyang, Characterizations of an X-ray detector based on a Zn<sub>2</sub>SiO<sub>4</sub> film. *Sensors and Actuators A*, 2015, vol. 236, pp. 98–103. DOI: 10.1016/j.sna.2015.08.022
6. Wen Chuang Wang, Yong Tao Tian, Kun Li, Er Yang Lu, Dong Shang Gong, Xin Jian Li, Capacitive humidity-sensing properties of Zn<sub>2</sub>SiO<sub>4</sub> film grown on silicon nanoporous pillar array. *Appl. Surface Sci.*, 2013, vol. 273, pp. 372–376 DOI: 10.1016/j.apsusc.2013.02.045
7. W. M. Yen, S. Shionoya, H. Yamamoto, Phosphor Handbook. Boca Raton: CRC Press, 2006. 1080 p.
8. I. F. Chang, G. A. Sai-Halasz, M. W. Shafer, Energy storage effect and retrieval in manganese doped zinc silicate. *J. Luminescence*, 1980, vol. 21, no. 3, pp. 323–327. DOI: 10.1016/0022-2313(80)90011-3
9. D. Y. Kong, M. Yu, C. K. Lin, X. M. Liu, J. Lin, J. Fang, Sol-gel synthesis and characterization of Zn<sub>2</sub>SiO<sub>4</sub>:Mn@SiO<sub>2</sub> spherical core-shell particles. *J. Electrochem. Soc.*, 2005, vol. 152, no. 9, pp. H146–H151. DOI: 10.1149/1.1990612
10. A. Osvet, M. Batentschuk, M. Milde, N. Lundt, C. Gellermann, S. Dembski, A. Winnacker, Ch. J. Brabec, Photoluminescent and storage properties of photostimulable core/shell type silicate nanoparticles. *Phys. Status Solidi C*, 2013, vol. 10, no. 2, pp. 180–184. DOI: 10.1002/pssc.201200515
11. U. Pal, P. Santiago, Controlling the morphology of ZnO nanostructures in a low-temperature hydrothermal process. *J. Phys. Chem. B*, 2005, vol. 109, no. 32, pp. 15317–15321. DOI: 10.1021/jp052496i
12. An-Jen Cheng, Yonhua Tzeng, Yi Zhou, Minseo Park, Tsung-hsueh Wu, Curtis Shannon, Dake Wang, Wonwoo Lee, Thermal chemical vapor deposition growth of zinc oxide

13. Haikuo Sun, Ming Luo, Wenjian Weng, Kui Cheng, Piyi Du, Ge Shen and Gaorong Han, Position and density control in hydrothermal growth of ZnO nanorod arrays through pre-formed micro/nanodots. *Nanotechnology*, 2008, vol. 19, no. 39, pp. 395602. DOI: 10.1088/0957-4484/19/39/395602
14. H. Amekura, Y. Sakuma, K. Kono, Y. Takeda, N. Kishimoto, Ch. Buchal, Luminescence from ZnO nanoparticles/SiO<sub>2</sub> fabricated by ion implantation and thermal oxidation. *Physica B: Condensed Matter.*, 2006, vol. 376–377, pp. 760–763. DOI: 10.1016/j.physb.2005.12.190
15. H. Amekura, N. Umeda, Y. Sakuma, O. A. Plaksin, Y. Takeda, N. Kishimoto, Zn and ZnO nanoparticles fabricated by ion implantation combined with thermal oxidation, and the defect-free luminescence. *Appl. Phys. Lett.*, 2006, vol. 88, no. 15, pp. 153119. DOI: 10.1063/1.2193327
16. B. Pandey, P. R. Poudel, D. L. Weathers, Formation of ZnO Nanoparticles by ZnO- and O- dual beam ion implantation and thermal annealing. *Jpn. J. Appl. Phys.*, 2012, vol. 51, no. 11S, pp. 11PG03. DOI: 10.1143/JJAP.51.11PG03
17. H. Amekura, N. Umeda, H. Boldyryeva, N. Kishimoto, Ch. Buchal, S. Mantl, Embedment of ZnO nanoparticles in SiO<sub>2</sub> by ion implantation and low-temperature oxidation. *Appl. Phys. Lett.*, 2007, vol. 90, no. 083102, pp. 083102. DOI: 10.1063/1.2709509
18. P. K. Kuiri, D. P. Mahapatra, Effects of annealing atmosphere on ZnO<sup>-</sup> ions-implanted silica glass: synthesis of Zn and ZnO nanoparticles. *J. Phys. D: Appl. Phys.*, 2010, vol. 43, no. 39, pp. 395404. DOI: 10.1088/0022-3727/43/39/395404
19. I. Muntele, C. Muntele, P. Thevenard, D. Ila, ZnO nanocluster formation in SiO<sub>2</sub> by low energy ion implantation. *Surface and Coatings Technology*, 2007, vol. 201, no. 19–20, pp. 8557–8559. DOI: 10.1016/j.surfcoat.2006.01.086

20. J. K. Lee, C. R. Tewell, R. K. Schulze, M. Nastasi, D. W. Hamby, D. A. Lucca, H. S. Jung, K. S. Hong, Synthesis of ZnO nanocrystals by subsequent implantation of Zn and O species. *Appl. Phys. Lett.*, 2005, vol. 86, no. 18, pp. 183111. DOI: 10.1063/1.1906304
21. B. Pandey, D. L. Weathers, Temperature dependent formation of ZnO and Zn<sub>2</sub>SiO<sub>4</sub> nanoparticles by ion implantation and thermal annealing. *Nuclear Instruments and Methods in Physics Research Section B: Beam Interactions with Materials and Atoms*, 2014, vol. 332, pp. 359–363. DOI: 10.1016/j.nimb.2014.02.096
22. A. S. Edelstein, R. C. Cammarata, *Nanomaterials: Synthesis, Properties and Applications*. New York; London: Taylor and Francis, 1996. 598 p.
23. C. Jagadish, S. J. Pearton, *Zinc oxide bulk, Thin films and nanostructures: processing, properties and applications*. Oxford: Elsevier, 2006. 600 p. DOI: 10.1016/B978-008044722-3/50000-2
24. V. L. Colvin, M. C. Schlamp, A. P. Alivisatos, Light-emitting diodes made from cadmium selenide nanocrystals and a semiconducting polymer. *Nature*, 1994, vol. 370, pp. 354–357. DOI: 10.1038/370354a0
25. Interactions of ions with matter. URL: <http://www.srim.org>
26. K. B. Eidelman, K. D. Shcherbachev, N. Y. Tabachkova, V. V. Privezentsev, Formation of nanoparticles containing zinc in Si(001) by ion-beam implantation and subsequent annealing. *Journal of Surface Investigation: X-Ray, Synchrotron and Neutron Techniques*, 2016, vol. 10, no. 3, pp. 597–602. DOI: 10.1134/S102745101603023X
27. J. R. Parsons, R. W. Balluffi, Displacement spike crystallization of amorphous germanium during irradiation. *J. Phys. Chem. Solids.*, 1964, vol. 25, no. 3, pp. 263–272. DOI: 10.1016/0022-3697(64)90106-4
28. A. G. Milnes, *Deep impurities in semiconductors*. New York: Wiley, 1973. 544 p.
29. The Materials Project. URL: <https://materialsproject.org>
30. O. Kubaschewski, C. Alcock, P. Spencer, *Materials thermochemistry*. Oxford; New York: Pergamon Press, 1993. 363 p.

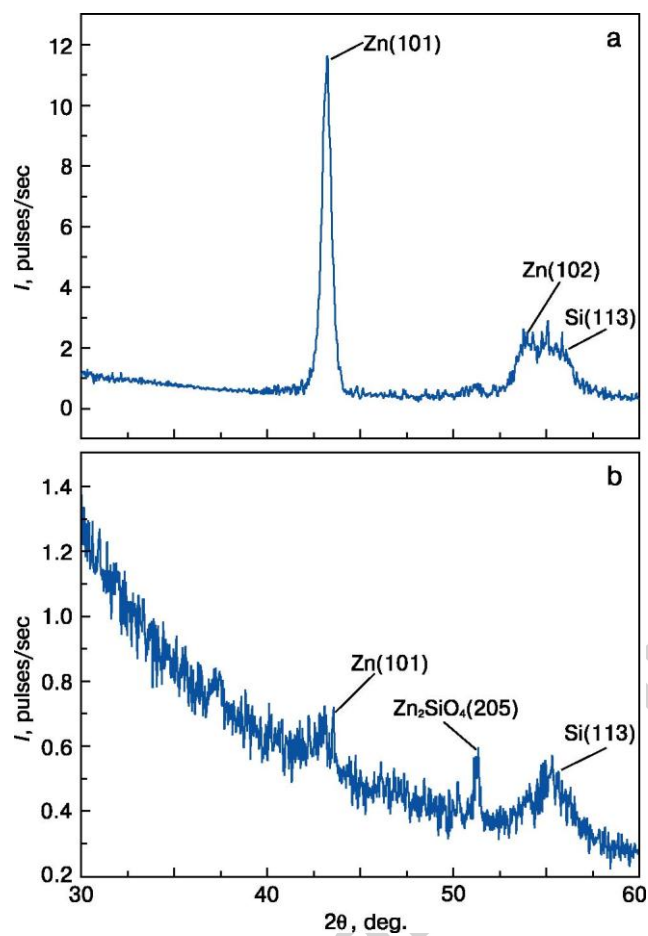
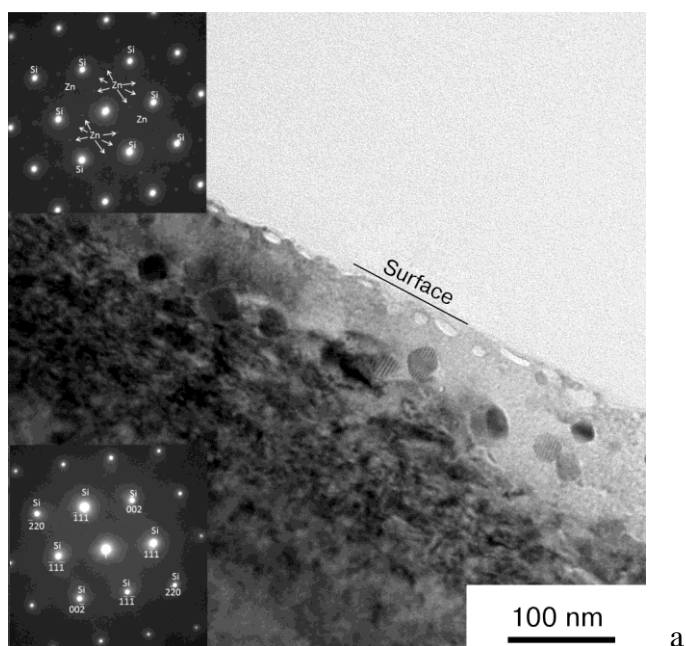
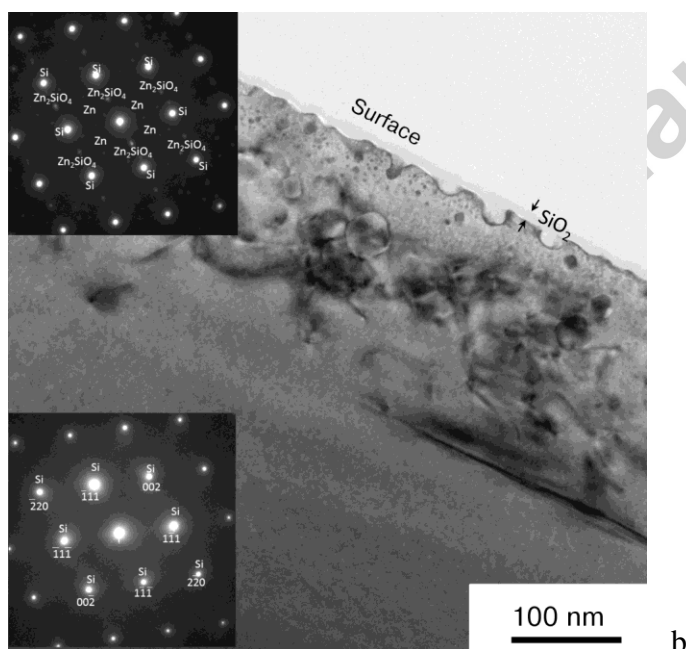


Figure 1. Surface silicon layer diffraction patterns after (a) Zn<sup>+</sup> implantation and (b) subsequent anneal at 800 °C.



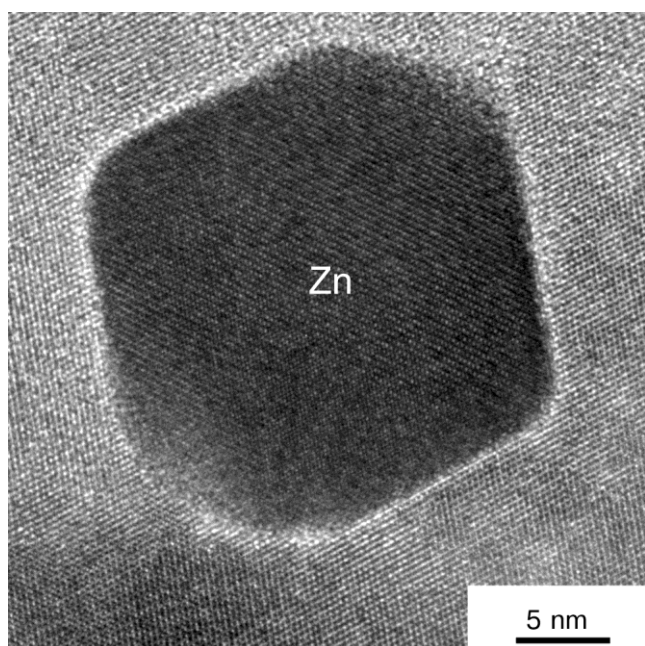
a



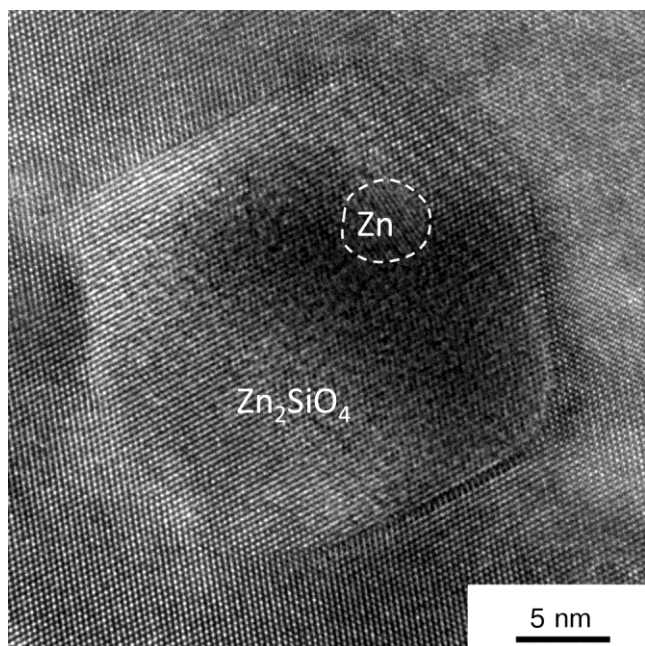
b

Figure 2. Surface silicon layer TEM images after (a) Zn<sup>+</sup> implantation and (b) subsequent anneal at 800 °C in dry air atmosphere. Insets: diffraction pattern of respective surface silicon layer areas.





a



b

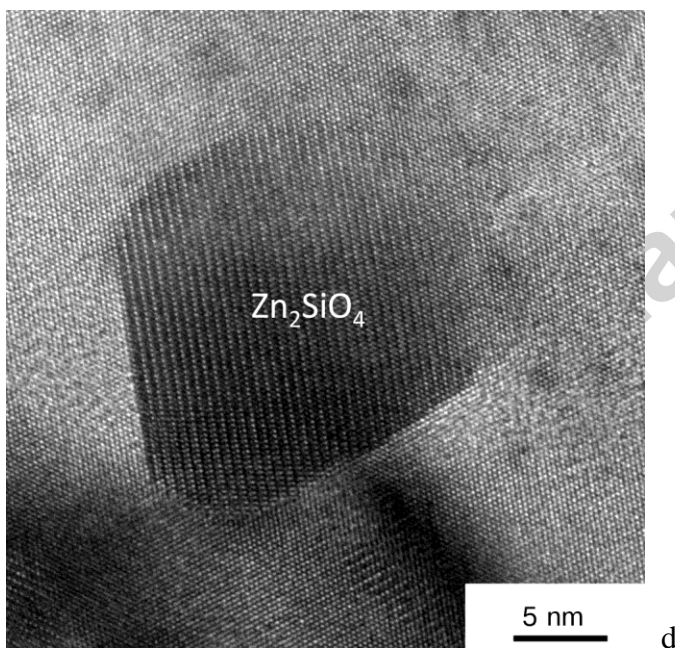
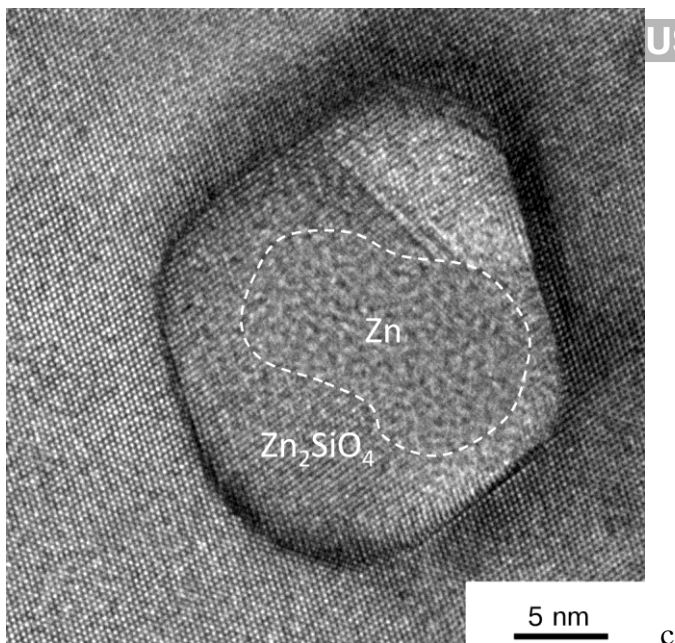


Figure 3. Nanoparticle phase composition evolution: *a*) Zn, (*b*, *c*) Core-Shell Zn-Zn<sub>2</sub>SiO<sub>4</sub> particles and (*d*) Zn<sub>2</sub>SiO<sub>4</sub>.

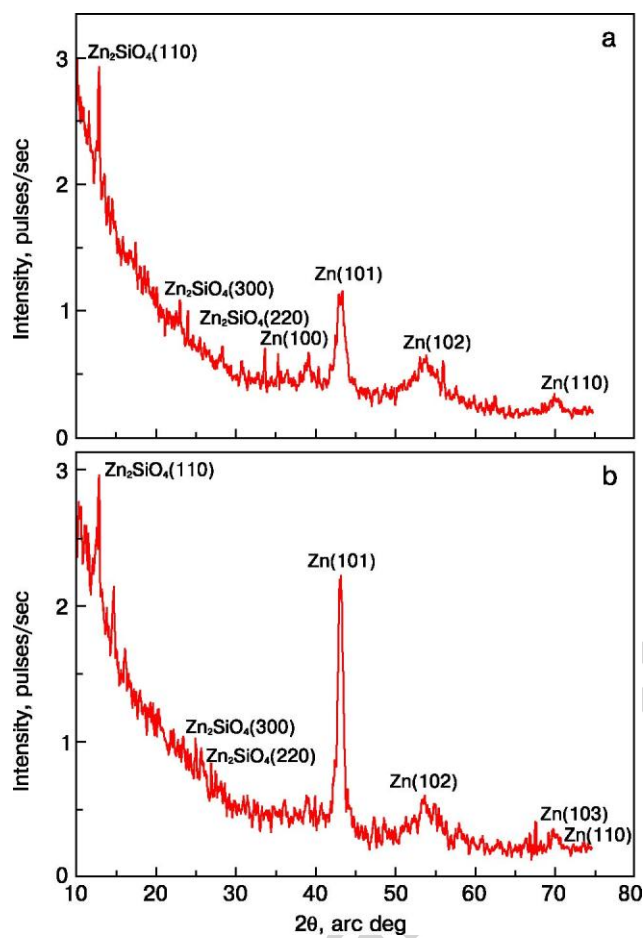


Figure 4. Surface silicon layer diffraction patterns after (a) sequential O<sup>+</sup> and Zn<sup>+</sup> implantation and (b) subsequent anneal at 800 °C.

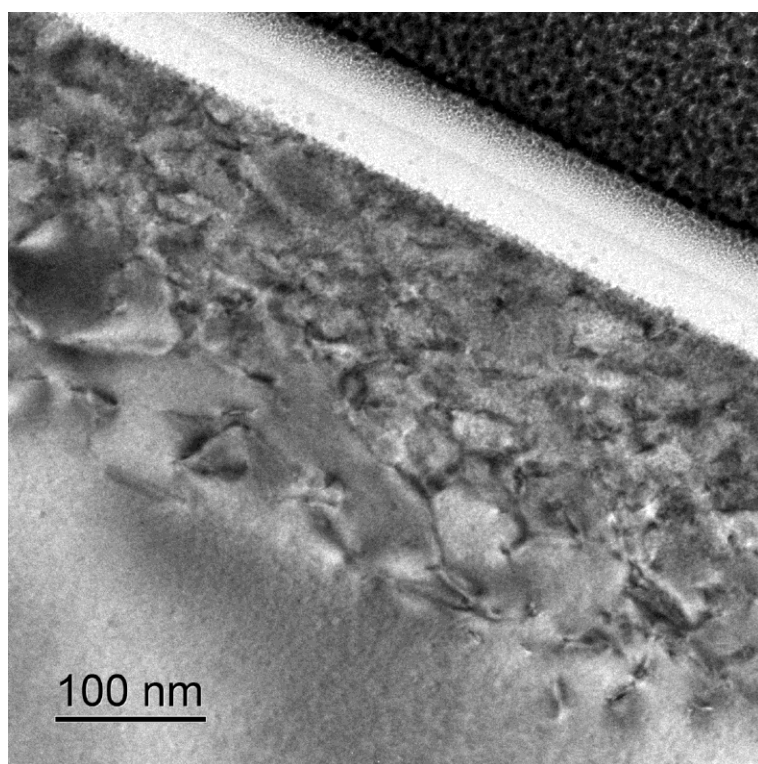
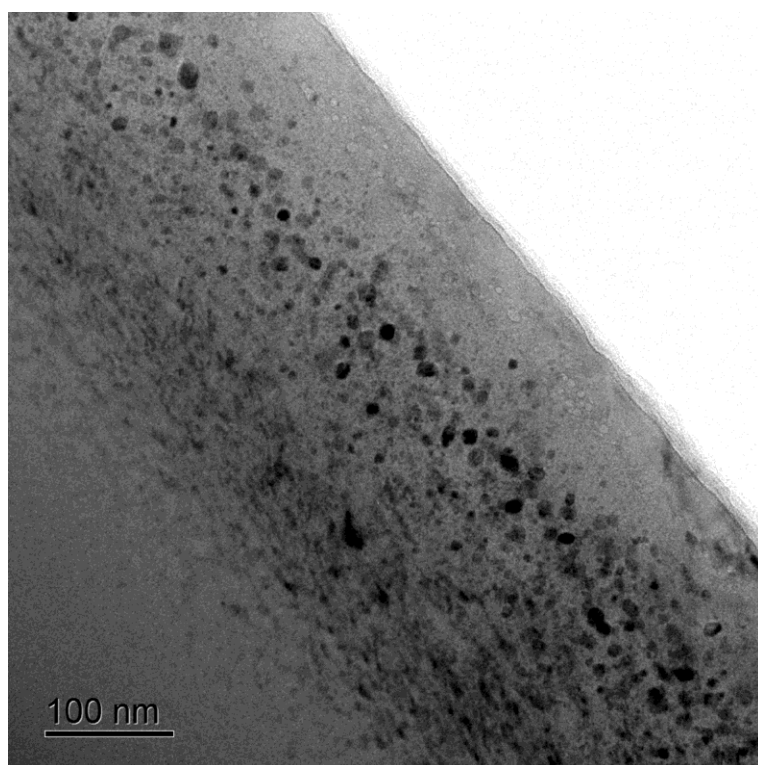


Figure 5. Surface silicon layer TEM images after (a) sequential  $O^+$  and  $Zn^+$  implantation and (b) subsequent anneal at 800 °C in dry air atmosphere. Insets: diffraction pattern of respective surface silicon layer areas.

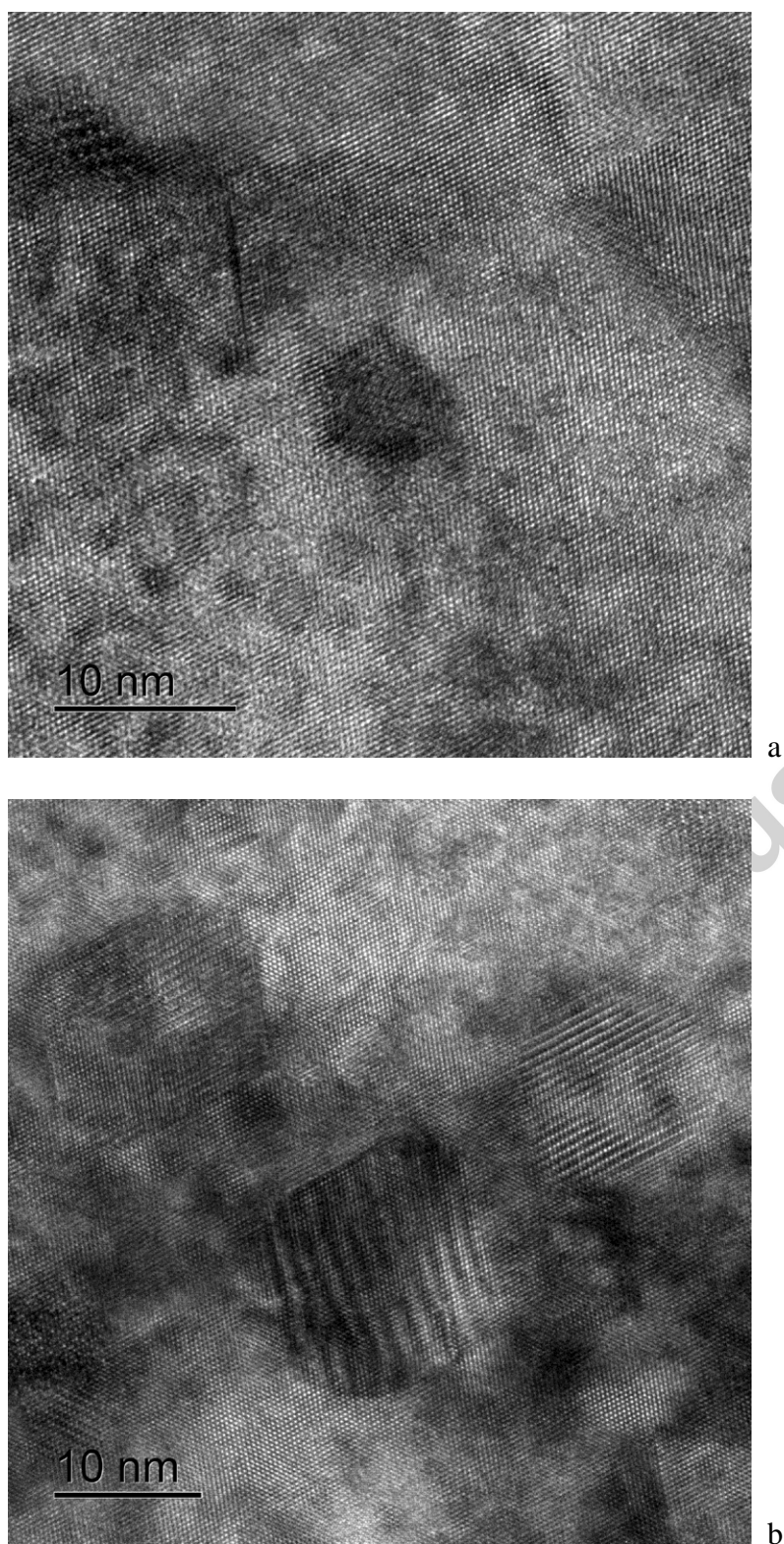


Figure 6. High resolution TEM images of particles in surface silicon layer after (a) sequential  $O^+$  and  $Zn^+$  implantation and (b) subsequent anneal at 800 °C in dry air atmosphere.